

# Geometry Effects at Atomic-Size Aluminium Contacts

U. Schwingenschlögl\*, C. Schuster

*Institut für Physik, Universität Augsburg, 86135 Augsburg, Germany*

---

## Abstract

We present electronic structure calculations for aluminium nanocontacts. Addressing the neck of the contact, we compare characteristic geometries to investigate the effects of the local aluminium coordination on the electronic states. We find that the Al  $3p_z$  states are very sensitive against modifications of the orbital overlap, which has serious consequences for the transport properties. Stretching of the contact shifts states towards the Fermi energy, leaving the system instable against ferromagnetic ordering. By spacial restriction, hybridization is locally suppressed at nanocontacts and the charge neutrality is violated. We discuss the influence of mechanical stress by means of quantitative results for the charge transfer.

*Key words:* density functional theory, electronic structure, stretched nanocontact, hybridization, charge neutrality

*PACS:* 71.20.-b, 73.20.-r, 73.20.At, 73.40.-c, 73.63.Rt

---

Atomic-size contacts can be prepared by means of scanning tunneling microscopy [1] or break junction techniques [2]. In each case, piezoelectric elements are used to stretch a wire with a precision of a few picometers until finally a single atom configuration is reached. Such contacts have attracted great attention over the last couple of years, in particular concerning their electrical transport properties. Since transport is restricted to a small number of atomic orbitals at the contact, conductance across nanocontacts strongly depends on the local electronic structure. An atomic-size constriction accommodates only a small number of conducting channels, which is determined by the number of valence orbitals of the contact atom. The transmission of each channel likewise is fixed by the local atomic environment. For a review on the quantum properties of atomic-size conductors see Agraït *et al.* [3].

---

\* Corresponding author. Fax: 49-821-598-3262

*Email address:* Udo.Schwingenschloegl@physik.uni-augsburg.de  
(U. Schwingenschlögl).

From the theoretical point of view, the electronic structure and conductance of nanocontacts and nanowires has been studied by ab initio band structure calculations. For aluminium contacts, investigations of the electronic states have been reported in [4,5,6,7], and the conductance has been addressed in [8,9,10,11,12,13,14,15,16]. In these studies various geometries have been used, which are assumed to model the local atomic structure of the contact in an adequate way. The breakage of an aluminium contact has been simulated by means of molecular dynamics calculations in [17,18,19], i.e. on the basis of realistic structural arrangements. However, despite such a large number of investigations, the literature lacks satisfactory reflections about the interrelations between the details of the crystal structure and the local electronic states at the nanocontact. In the present letter we will deal with this point by comparing characteristic contact geometries, including stretched configurations.

In a previous work [20] we have demonstrated that hybridization between Al  $3s$  and  $3p$  states is strongly suppressed at aluminium nanocontacts due to directed bonds at the neck of the contact. We therefore expect the system to be very sensitive against modifications of the orbital overlap coming along with the specific contact geometry. As a consequence, structural details are important for the electrical transport, since hybridization effects can play a critical role for transport properties of atomic-size contacts and interfaces [21,22,23]. In particular, stretching of the nanocontact alters the chemical bonding and thus may lead to unexpected electronic features. We will show that it is mandatory to account for the very details of the contact geometry in order to obtain adequate results from electronic structure calculations.

The band structure results presented subsequently are obtained within density functional theory and the generalized gradient approximation. We use the WIEN2k program package, a state-of-the-art full-potential code based on a mixed lapw and apw+lo basis [24]. In our calculations the charge density is represented by  $\approx 150000$  plane waves and the exchange-correlation potential is parametrized according to the Perdew-Burke-Ernzerhof scheme. Moreover, the mesh for the Brillouin zone integration comprises between 75 and 102 points in the irreducible wedge. While Al  $1s$ ,  $2s$ , and  $2p$  orbitals are treated as core states, the valence states comprise Al  $3s$  and  $3p$  orbitals. The radius of the aluminium muffin-tin spheres amounts to 2.6 Bohr radii.

Our calculations rely on two characteristic contact geometries, which we introduce in the following. On the one hand, we address a configuration where a single Al atom is connected to planar Al units on both sides, each consisting of seven atoms in a hexagonal arrangement with fcc [111] orientation. The central sites of these planar units lie on top of the contact atom, thus giving rise to linear  $\sigma$ -type Al-Al bonds along the  $z$ -axis. For this reason, we call the first geometry under consideration the *linear contact configuration*. The finite Al units are connected to Al *ab*-planes of infinite extension, which enables us

to apply periodic boundary conditions. We note that the contact Al site in this linear geometry, due to its two nearest neighbours, resembles the essential structural features of atoms in a monostrand nanowire [20].

On the other hand, we study an Al atom sandwiched between two pyramidal Al electrodes in fcc [001] orientation, which we call the *pyramidal contact configuration*. To be specific, the contact Al site has four crystallographically equivalent nearest neighbours on both sides, which prohibits  $\sigma$ -type Al-Al bonding via the  $3p_z$  orbitals along the  $z$ -axis. Whereas the second pyramidal layer comprises nine atoms, the third layer off the contact extends infinitely on account of periodic boundary conditions.

For both contact configurations, a convenient choice for the bond lengths and bond angles is given by the bulk (fcc) aluminium values, therefore by interatomic distances of 2.86 Å. Mechanical stress can increase this bond length at the nanocontact, which we simulate by interatomic distances of 3.95 Å for the linear and 3.62 Å for the pyramidal contact configuration. In both cases, only the bond lengths between the contact Al site and its nearest neighbours are changed with respect to the fcc setup. Structural relaxation of the electrodes due to the elongated contact bonds plays a minor role.

For bulk aluminium it is well established that the formal Al  $3s^23p^1$  electronic configuration is seriously interfered by hybridization effects, giving rise to a prototypical  $sp$ -hybrid system. However, the situation changes dramatically when covalent bonding is no longer isotropic but restricted to specific directions, as for an atomic-size contact. Partial Al  $3s$ ,  $3p_z$ , and  $3p_x$  densities of states (DOS) as calculated for the Al site at the neck of our linear contact configuration are shown in figure 1. By symmetry,  $p_x$  and  $p_y$  states are degenerate. While most of the occupied states are of  $3s$  type, the  $3p$  states dominate at energies above the Fermi level. Because hardly any contribution of  $3s$  and  $3p$  states is found at energies dominated by the other states, respectively, evolution of hybrid orbitals and an interpretation in terms of  $sp$ -hybrid states is precluded. Most  $3p$  electrons occupy the  $p_z$  orbital, which is oriented along the principal axis of the contact and therefore mediates  $\sigma$ -type orbital overlap. Because neither  $3s$  nor  $3p_x$  states give rise to significant contributions to the DOS at the Fermi energy, chemical bonding is well characterized in terms of directed  $3p_z$  bonds.

When the Al-Al bond length is stretched from 2.86 Å to 3.95 Å at the nanocontact, the central Al site decouples from its neighbours. Its electronic states hence become more atom-like, which is clearly visible for the  $3s$  states in figure 1. Smaller band widths and sharper DOS structures likewise are obvious for the  $3p_x$  states. Finally, for the  $3p_z$  symmetry component we observe a shift of states from lower energies to the Fermi level and from higher energies to a new structure at about 2 eV. The DOS at the Fermi energy increases

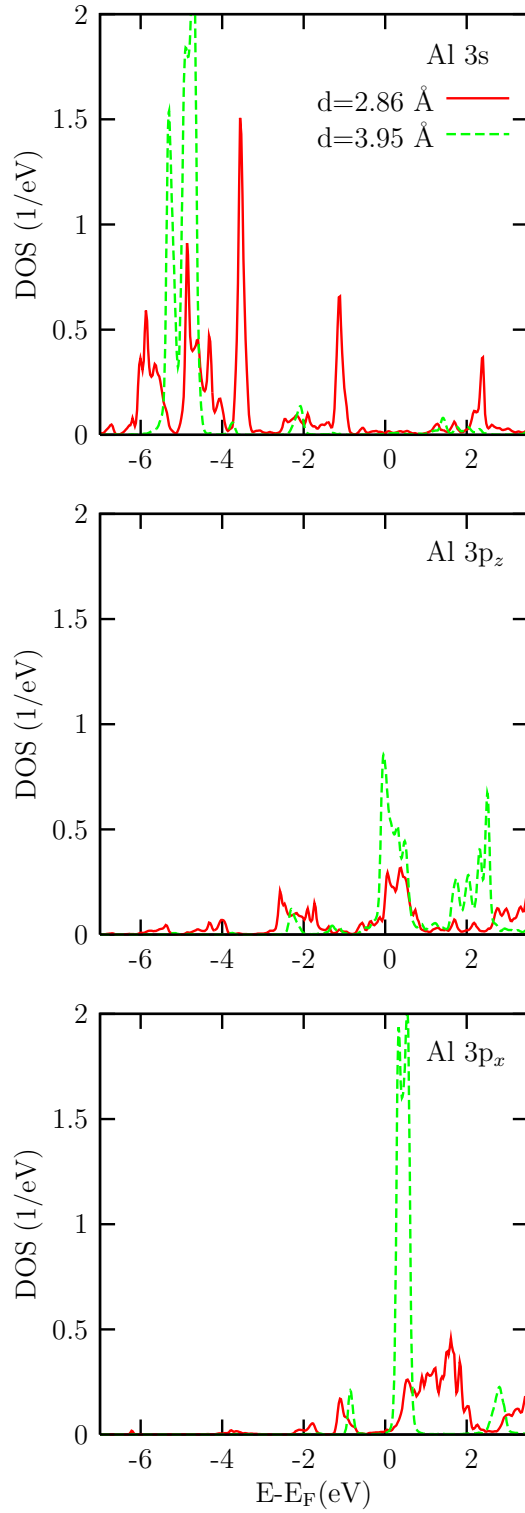


Fig. 1. Partial Al  $3s$ ,  $3p_z$ , and  $3p_x$  densities of states for the contact aluminium site in the linear contact configuration.

configuration	bond length	charge transfer
linear	2.86 Å	0.51
	2.97 Å	0.54
	3.08 Å	0.57
	3.33 Å	0.59
	3.58 Å	0.62
	3.95 Å	0.63
pyramidal	2.86 Å	0.22
	3.22 Å	0.53
	3.62 Å	0.61
	4.04 Å	0.66

Table 1  
Net charge transfer off the contact aluminium site.

significantly.

Turning to the occupation of the valence orbitals, the decoupling of the contact Al site comes along with a reduction of charge, amounting to 0.13 electrons. In general, the  $p_x/p_y$  atomic orbital does not mediate chemical bonding due to the spacial restriction of the crystal structure. Its occupation thus is strongly reduced and we cannot expect local charge neutrality. Calculated values for the net charge transfer off the contact Al site, as compared to bulk aluminium, are given in table 1 for bond lengths between 2.86 Å and 3.95 Å.

Figure 2 shows partial Al  $3s$ ,  $3p_z$ , and  $3p_x$  densities of states for the pyramidal contact configuration. As compared to the linear case fundamental differences are found. For an Al-Al bond length of 2.86 Å we now have a finite Al  $3s$  DOS at the Fermi energy. The same is true for the  $3p_z$  states, whereas the  $3p_x$  DOS almost vanishes. Again,  $p_x$  and  $p_y$  states are degenerate by symmetry. While most of the occupied states still are of  $3s$  type, contributions of the  $3p$  states are larger than for the linear contact configuration. Chemical bonding therefore is more isotropic, which is reflected by larger band widths. As expected from the contact geometry,  $\sigma$ -type bonding via the  $3p_z$ -orbital is significantly reduced. Due to increased hybridization between the  $3s$  and the three  $3p$  orbitals, all these states can participate in the electrical transport. Figure 3 illustrates the differences in the electronic structure at the linear and pyramidal contact by means of electron density maps. In each case, the density map covers the plane of the central Al site, where the principal axis of the contact runs from left to

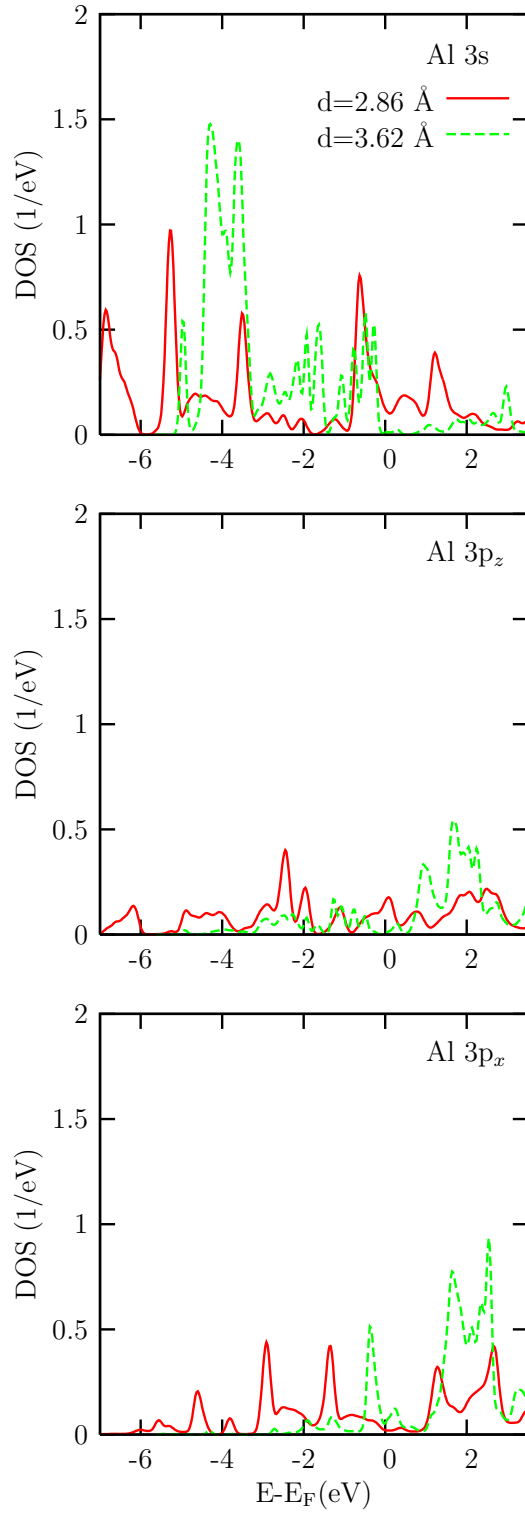


Fig. 2. Partial Al 3s, 3p<sub>z</sub>, and 3p<sub>x</sub> densities of states for the contact aluminium site in the pyramidal contact configuration.

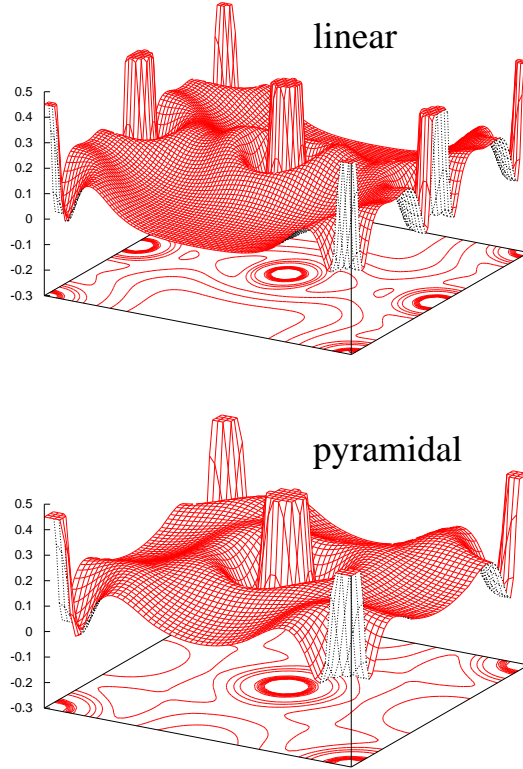


Fig. 3. Electron density maps for the neck of the linear and pyramidal contact.

right.

Stretching of the contact by increasing the Al-Al bond length from 2.86 Å to 3.62 Å has similar effects as for the linear contact configuration. The decoupling of the central Al site from the pyramidal electrodes results in smaller band widths and sharper DOS structures for the  $3s$ ,  $3p_z$ , as well as  $3p_x$  states, see figure 2. In addition, the  $3p_z$  and  $3p_x$  states shift to higher energies, giving rise to pronounced DOS structures near 2 eV. Due to the reduced band width, the  $3s$  and  $3p_z$  DOS disappears almost completely in the vicinity of the Fermi energy. As concerns the  $3p_z$  states, the pyramidal geometry thus shows the opposite behaviour than the linear geometry. Since the Al  $3p_z$  states mediate the main part of the orbital overlap across the nanocontact, they are very sensitive against changes in the crystal structure. Structural rearrangement during the breakage of an aluminium nanocontact or nanowire consequently should have serious effects on the electrical transport, such as modulation of the conductance.

Elongated bonds again are accompanied by a decline of charge at the contact. However, the value of 0.39 electrons net charge transfer off the central Al site is larger than in the linear case. This traces back to the fact that reduction of hybridization on stretching is more efficient for the pyramidal geometry, since for the linear geometry hardly any hybridization is left right from the

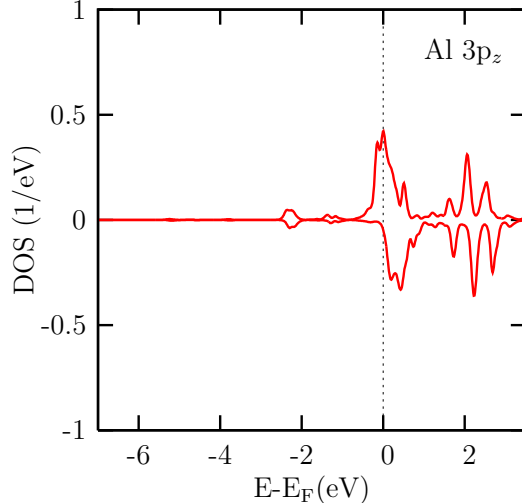


Fig. 4. Spin majority and minority Al  $3p_z$  densities of states for the contact aluminium site in the stretched linear contact configuration ( $d = 3.95 \text{ \AA}$ ).

beginning. Accordingly, smaller values for the net charge transfer are found in the pyramidal case, see table 1.

We next show that the remarkable increase of the Al  $3p_z$  DOS at the Fermi energy on stretching the linear contact configuration leads to an instability against ferromagnetic ordering. A spontaneous magnetization of simple metal nanowires has been predicted by Zabala *et al.* [4]. These authors have demonstrated the instability in explicit calculations for an aluminium nanowire, using a stabilized jellium model. For Al-Al bond lengths of  $d = 3.95 \text{ \AA}$  at the neck of our contact, we hence have performed spin polarized electronic structure calculations, yielding a stable ferromagnetic solution. Figure 4 displays the corresponding spin majority and minority densities of states for the contact Al site. The local spin splitting of about 0.2 eV is connected to an energy gain of 5.5 mRyd. Moreover, the magnetic moment amounts to  $0.1 \mu_B$ , which is significantly smaller than the  $0.68 \mu_B$  reported by Zabala *et al.* [4] for an infinite nanowire. However, Delin *et al.* [6] have shown for Pd nanowires that the spontaneous magnetization decreases rapidly for short chains. Only the linear contact configuration is subject to a magnetic instability on stretching. For the pyramidal geometry, of course, magnetism cannot be expected, compare the spin degenerate DOS curves in figure 2.

In conclusion, we have studied the electronic structure of aluminium nanocontacts by means of band structure calculations within density functional theory. Taking into account the details of the crystal structure, we have discussed the electronic features of prototypical contact geometries (linear versus pyramidal). Our calculations result in two largely different scenarios. In particular, the Al  $3p_z$  states are strongly affected by modifications of the chemical bonding. If  $\sigma$ -type bonding via the  $3p_z$  orbitals is dominant because of direct orbital



overlap across the contact, *sp*-type hybridization is almost completely suppressed and only Al  $3p_z$  states remain at the Fermi energy [20]. Otherwise, if the bonding is more isotropic for geometrical reasons, the Al  $3s$  states likewise have to be taken into account. The diverse behaviour of the linear and pyramidal geometry becomes even more pronounced when the contact is stretched. Whereas in the linear case the Al  $3p_z$  DOS at the Fermi energy increases, which even yields a ferromagnetic instability, it vanishes in the pyramidal case, leaving the system insulating. As a consequence, the structural details of the contact are expected to strongly influence the electrical transport. Because of structural rearrangements, they are particularly relevant for the breakage of a nanocontact or nanowire.

## Acknowledgements

We thank U. Eckern and P. Schwab for helpful discussions and the Deutsche Forschungsgemeinschaft for financial support (SFB 484).

## References

- [1] Pascual J.I., Méndez J., Gómez-Herrero J., Baró A.M., and García N., Phys. Rev. Lett. 71 (1993) 1852.
- [2] Scheer E., Joyez P., Esteve D., Urbina C., and Devoret M.H., Phys. Rev. Lett. 78 (1997) 3535.
- [3] Agraït N., Levi-Yeyati A., and van Ruitenbeck J.-M., Phys. Rep. 377 (2003) 81.
- [4] Zabala N., Puska M.J., Ayuela A., Raebiger H., and Nieminen R.M., J. Magn. Mater. 249 (2002) 193.
- [5] Ribeiro F.J., and Cohen M.L., Phys. Rev. B 68 (2003) 035423.
- [6] Delin A., Tosatti E., and Weht R., Phys. Rev. Lett. 92 (2004) 057201.
- [7] Delin A. and Tosatti E., J. Phys.: Condens. Matter 16 (2004) 8061.
- [8] Levy-Yeyati A., Martín-Rodero A., and Flores F., Phys. Rev. B 56 (1997) 10369.
- [9] Cuevas J.C., Levi-Yeyati A., and Martín-Rodero A., Phys. Rev. Lett. 80 (1998) 1066.
- [10] Cuevas J.C., Levi-Yeyati A., Martín-Rodero A., Bollinger G.R., Untiedt C., and Agraït N., Phys. Rev. Lett. 81 (1998) 2990.
- [11] Kobayashi N., Brandbyge M., and Tsukada M., Phys. Rev. B 62 (2000) 8430.

- [12] Palacios J.J., Pérez-Jiménez A.J., Louis E., SanFabián E., and Vergés J.A., Phys. Rev. B 66 (2002) 035322.
- [13] Thygesen K.S., and Jacobsen K.W., Phys. Rev. Lett. 91 (2003) 146801.
- [14] Lee H.-W., Sim H.-S., Kim D.-H., and Chang K.J., Phys. Rev. B 68 (2003) 075424.
- [15] Okano S, Shiraishi K., and Oshiyama A., Phys. Rev. B 69 (2004) 045401.
- [16] Sasaki T., Egami Y., Ono T., and Hirose K., Nanotechnology 15 (2004) 1882.
- [17] Hasmy A., Medina E., and Serena P.A., Phys. Rev. Lett. 86 (2001) 5574.
- [18] Hasmy A., Pérez-Jiménez A.J., Palacios J.J., García-Mochales P., Costa-Krämer J.L., Díaz M., Medina E., and Serena P.A., Phys. Rev. B 72 (2005) 245405.
- [19] Pauly F., Dreher M., Viljas J.K., Häfner M., Cuevas J.C., and Nielaba P., arXiv:cond-mat/0607129.
- [20] Schwingenschlögl U. and Schuster C., Chem. Phys. Lett. 432 (2006) 245.
- [21] Schmitt T., Augustsson A., Nordgren J., Duda L.-C., Höwing J., Gustafsson T., Schwingenschlögl U., and Eyert V., Appl. Phys. Lett. 86 (2005) 064101.
- [22] Schwingenschlögl U. and Schuster C., Chem. Phys. Lett. 435 (2007) 100.
- [23] Schwingenschlögl U. and Schuster C., Europhys. Lett. 37 (2007) 37007.
- [24] Blaha P., Schwarz K., Madsen G., Kvasicka D., and Luitz J., WIEN2k: An augmented plane wave + local orbitals program for calculating crystal properties, Vienna University of Technology, 2001.